Journal of Thermal Analysis and Calorimetry, Vol. 95 (2009) 1, 59–62

THERMAL AND STRUCTURAL INVESTIGATION OF Er:$YAl_3(BO_3)_4$ NANOCRYSTALLINE POWDERS

Cynthia R. Ferrari[1,2*], *Maria Baccia*[2], *A. Ibanez*[2] *and A. C. Hernandes*[1]

[1]Instituto de Física de São Carlos, Universidade de São Paulo, São Carlos, Caixa Postal 369, 13560-970, SP, Brazil
[2]Institut Néel, CNRS et UJF, UPR 2940, 25 Avenue des Martyrs, BP 166, 38042 Grenoble, France

Pure Er:YAB (Er:$YAl_3(BO_3)_4$) nanometer-sized crystalline powder was produced from low cost chemical route, the polymeric precursor method. The initial homogeneous solutions were heat treated from 200 to 700°C under oxygen atmosphere and the unique crystalline phase was synthesized at around 1150°C. The thermal treatments and the initial stoichiometry play a very important role on the Er:YAB preparation. The thermal events of amorphous precursor resins and the crystallization process up to phase formation were investigated.

Keywords: *structural stability, thermal analysis, YAB crystal, yttrium aluminum borate*

Introduction

Yttrium aluminum borate, $YAl_3(BO_3)_4$, crystals are grown from the flux method and they are not easy to obtain in adequate size and optical quality. In addition, significant amount of impurities are present in YAB crystals coming from the flux (Mo for example) [1, 2]. For this reason, we have recently investigated the preparation of fine powders of YAB doped with Er^{3+} for the development of phosphor powders or YAB transparent ceramics. Our final objective is to propose new non-cubic ceramics for optics which could be sintered at lower temperature than others ceramic oxides.

YAB has a trigonal structure of huntite $CaMg_3(CO_3)_4$ with the space group R32 [3]. Al^{3+} ions occupy the octahedral site in the crystal lattice while borons are arranged in sheets of $[BO_3]^{3-}$ groups. The active rare-earth (RE) dopant replaces the Y^{3+} ion, which occupies the trigonal prismatic site [4].

The Y_2O_3–$3Al_2O_3$–$4B_2O_3$ system from solid-state reactions was investigated by Beregi *et al.* [5] using infrared absorption spectroscopy and X-ray diffraction and by Madarász *et al.* [6] using combined DTA and X-ray diffraction measurements. They were interested to understanding the chemical process in order to improve the crystal growth techniques. Nd^{3+}:YAB was also studied by Jung *et al.* [7] to know the decomposition temperature in function of the neodymium content.

In this paper, we report the chemical synthesis and structural evolution of Er:YAB nanopowder obtained from the polymeric precursor method (Modified Pechini method). An excess of boric acid during the chemical synthesis was used in order to balance the stoichiometry loss between 830 and 930°C as observed earlier [8, 9].

This study was carried out through thermal analysis, X-ray diffraction and transmission electron microscopy techniques. These results contribute to the better understanding of this complex system and for the preparation of pure YAB nanometer-sized powders.

Experimental

The flow chart in Fig. 1 illustrates the procedure involved in the preparation of YAB powders. The synthesis of fine powders was carried out by the polymeric precursor method which is based on the complexation of metal cations by carboxylic acid (citric acid) followed by the polymerization process (polyesterification reactions) using a polyalcohol (*D*-sorbitol) to form a three-dimensional polymeric network. The resin synthesis was achieved by dissolving the precursors $Y(NO_3)_3 \cdot 6H_2O$ (Aldrich 99.9%), $Er(NO_3)_3 \cdot 5H_2O$ (Aldrich 99.9%) and $Al(NO_3)_3 \cdot 9H_2O$, (Prolabo 98%) in an aqueous solution of citric acid monohydrate ($C_5O_7H_8.H_2O$, Aldrich 99.5%) at 80°C, to form metallic citrates. This solution of metallic citrates was added to another aqueous solution of *d*-sorbitol ($C_6O_6H_{14}$, Aldrich 99.5%) and boric acid (H_3BO_3, Carlo Erba 99.8%).

The polymerization takes place at 120°C under constant stirring. The amount of citric acid is determined by the molar ratio citric acid/metals and was fixed, in this work, to 3:1. The citric acid/*D*-sorbitol mass ratio was fixed to 3:2. The dried gels and resins were calcinated under an oxygen-rich atmosphere

---

[*] Author for correspondence: cyferrari@if.sc.usp.br

1388–6150/$20.00

Akadémiai Kiadó, Budapest, Hungary
Springer, Dordrecht, The Netherlands

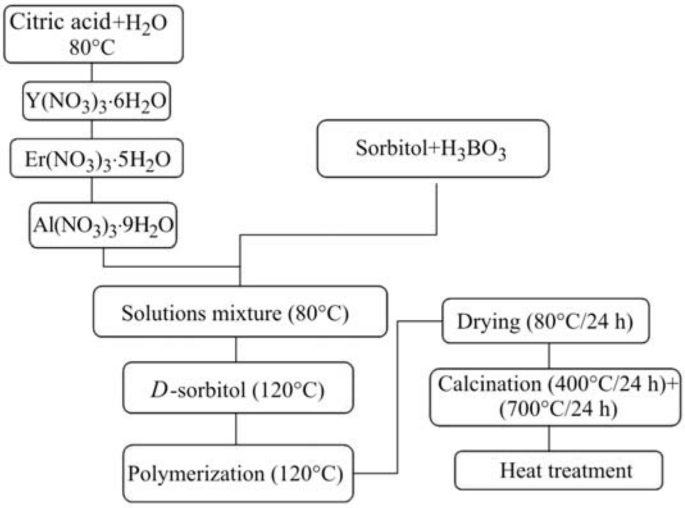

Fig. 1 Flow chart of $Y_{0.9}Er_{0.1}Al_3B_{4.5}O_{12.75}$ powder preparation using the polymeric precursor method

at 400°C/24 h and 700°C/24 h with a heating rate of 5°C min^{-1} resulting to organic-free fine powders. Then, white nanometer-sized powders corresponding to the well-crystallized Er:YAB phase was obtained at 1150°C. The chemical reactions from the initial amorphous resin to the Er:YAB single crystallized fine powders were previously studied [9]. In these studies, it was observed that a small loss of boron occurs during the heat treatment. The loss of boron was analysed by thermogravimetry experiments (see in results section) and indicated the loss around 10 mol% of B_2O_3. In all experiments we corrected the boron sublimation using a B_2O_3 excess.

The mass loss, glass transition temperature and the crystallization processes of the powders heat treated only at 400°C/24 h were investigated by coupled thermal analyses (PerkinElmer), thermogravimetry (TG) and differential thermal analysis (DTA) techniques. Measurements were performed with a heating rate of 10°C min^{-1} from room temperature up to 1200°C, under a continuous flow of O_2 (80 mL min^{-1}) and mass samples were around 30 mg. The reference material for DTA was Al_2O_3.

The evolution of the crystalline phases as a function of the heat treatment temperature was studied by X-ray diffraction (XRD) at room temperature. These XRD measurements were performed in transmission geometry on a Siemens D-5000 diffractometer equipped with a nickel filter and a graphite monochromator. The radiation applied was CuK_α (λ=1.5406 Å), operating at 40 kV and 50 mA. XRD scans were made from 10 to 60° in 2θ with steps of 0.016°. Finally, morphology, particle size and crystallinity were analyzed by transmission electronic microscopy (TEM, Philips CM 300).

Results and discussion

Figure 2 shows the TG curve where one can observe a first loss (16.5%) extended from room temperature (*RT*) to around 430°C corresponding to the elimination of water and organic phases like citrates. The second loss of 7.6% between 430 and 600°C corresponds to residual organic phase and water more strongly linked to the inorganic network (–OH groups) and the third loss of 2.8% (up to 800°C), the more stable organic groups (carbonates). At higher temperatures, from 800 to 1040°C the loss of 6.3% is mainly due a B_2O_3 departure, which occurs simultaneously to events of crystallization (also Fig. 3). The B_2O_3 loss allows us to currently specify the starting compositions of the different precursors which correspond to approximately 10% molar excess of B_2O_3. Besides, the initial resin was heat-treated at 700°C during 24 h to enhance the alumino-borate network densification which better trapp B_2O_3 thus avoiding its sublimation.

In the DTA curve (Fig. 3), the T_g transition is not well-defined at around 700°C. At higher temperature, three exothermic peaks between 800 and 1000°C, due to several phase crystallizations or structural transi-

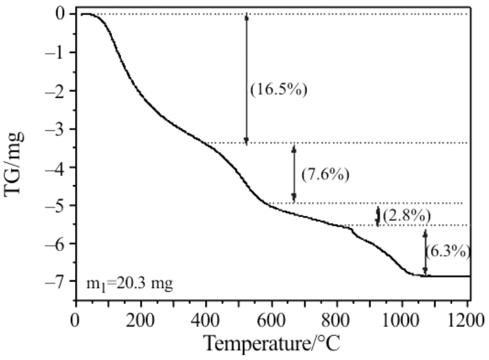

Fig. 2 TG curve of $Y_{0.9}Er_{0.1}Al_3B_{4.5}O_{12.75}$ powder previously calcined at 400°C for 24 h

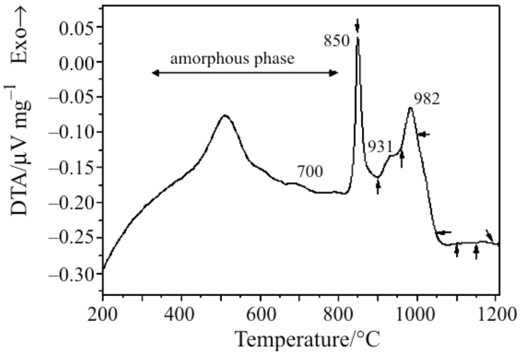

Fig. 3 DTA curves of $Y_{0.9}Er_{0.1}Al_3B_{4.5}O_{12.75}$ powder previously calcined at 400°C for 24 h. (Calcination and DTA measurements in oxygen-rich atmosphere. The small arrows indicate the temperatures where the XRD measurements were taken.)

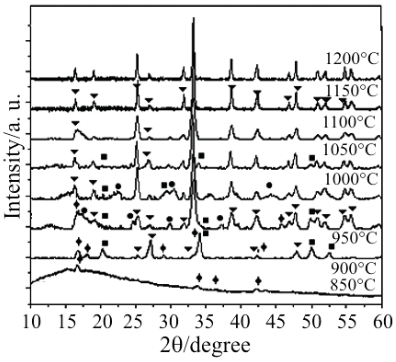

Fig. 4 XRD patterns of $Y_{0.9}Er_{0.1}Al_3B_{4.5}O_{12.75}$ powders previously calcined at 400°C/24 h and 700°C/24 h and heat treated at different temperatures by heating and followed cooling at 5°C min^{-1} in oxygen-rich atmosphere

tions. These crystallization peaks are centred at around 848, 931 and 982°C, respectively.

The crystalline phases arising from the crystallization peaks were identified by XRD measurements. Figure 4 illustrates the XRD pattern of powders previously calcined at 400°C/24 h and 700°C/24 h and heat treated then at different temperatures, specified above each XRD pattern. For Er:YAB preparation, it was observed that the pure phase formation is favoured when the initial resin is previously heat treated at low temperatures (400 and 700°C) for the total organic precursor removal followed by the final heat treatment at 1150°C in oxygen-rich atmosphere.

The specified annealing temperatures in Fig. 4 were selected between the exothermic crystallization peaks of DTA curves (Fig. 3) in order to identify the different phase formations. Table 1 summarizes the phase evolution as a function of temperature.

From the DTA and XRD measurements it is possible to note that at 800°C the powder remained amorphous. In the DTA curve the first exothermic peak corresponds to $Al_4B_2O_9$ crystallization in agreement with the XRD pattern heated to 850°C. At 950°C, presence of $(Y,Er)BO_3$, Er:YAB and $YAl_2B_4O_{10.5}$ crystalline phases can be seen. Then, the second large exothermic peak centred at 931°C corresponds to the partial transformation of $Al_4B_2O_9$ phase and amorphous part into $(Y,Er)BO_3$, Er:YAB and $YAl_2B_4O_{10.5}$ crystalline phases. Between 1000 and 1050°C, a significant increase of Er:YAB diffraction peaks is coupled to the decrease of those of $(Y,Er)BO_3$ and $YAl_2B_4O_{10.5}$ compounds. Thus, the third exothermic peak centred at 982°C is due to the Er:YAB crystallization. Indeed, between 1000 and 1100°C, the $YAl_2B_4O_{10.5}$ and $(Y,Er)BO_3$ phases reacts with an amorphous contents, enriched in boron and aluminium to form the Er:YAB phase, in good agreement with the DTA results in which the crystallization process finishes at 1070°C. These phase transformations are completed above 1150°C to obtain pure Er:YAB crystalline phase.

Crystallization of YAB powders previously reported by Madarász *et al.* [6] showed the YBO_3 formation due to the Y_2O_3–B_2O_3 reaction in the 700–980°C range. They also reported the occurrence of $Al_4B_2O_9$ phase formation between 900 and 1000°C while the $YAl_3(BO_3)_4$ was obtained between 800 and 1150°C. These results partially corroborates with the ones above discussed.

Based on the literature [5, 6], and on thermal analyses and XRD measurements the following chemical reactions can be proposed to obtain the final crystalline Er:YAB phase starting from the $6[(Y_{0.9}Er_{0.1})Al_3B_{4.5}O_{12.75}]$ initial amorphous composition:

- 800–850°C

$$8a\text{-}Al_2O_3+4a\text{-}B_2O_3\rightarrow 4c\text{-}Al_4B_2O_9 \quad (1)$$

$$a\text{-}Al_2O_3+a\text{-}B_2O_3\rightarrow 2a\text{-}AlBO_3 \quad (2)$$

Table 1 Phase formation observed in the XRD patterns for $Y_{0.9}Er_{0.1}Al_3B_{4.5}O_{12.75}$ starting compositions

Temperature/°C	Phase
800	amorphous
850	$Al_4B_2O_9$ (◆, JCPDS No. 09-0158)
900	$Al_4B_2O_9$ (◆)+$(Y,Er)BO_3$ (■, JCPDS No. 74-1929 and No. 74-1935)+Er:YAB (▼, JCPDS No. 72-1978)
950	$Al_4B_2O_9$ (◆)+YBO_3 and $ErBO_3$ (■)+Er:YAB (▼)+$YAl_2B_4O_{10.5}$ (●, US5043308 Patent) [10]
1000–1100	$(Y,Er)BO_3$ (■)+Er:YAB (▼)+$YAl_2B_4O_{10.5}$ (●)
1150–1200	Er:YAB (▼)

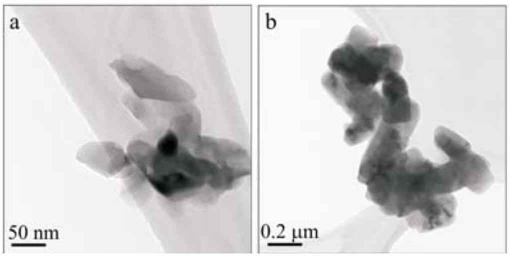

Fig. 5 Transmission electron micrographs of $Y_{0.9}Er_{0.1}Al_3B_{4.5}O_{12.75}$ nanometric powders, a – amorphous powder and b – crystalline powder Er:YAB

$$3a\text{-}(Y,Er)_2O_3+3a\text{-}B_2O_3\rightarrow 6c\text{-}(Y,Er)BO_3 \quad (3)$$

- 900–1100°C

$$c\text{-}Al_4B_2O_9+2c\text{-}(Y,Er)BO_3+2a\text{-}B_2O_3\rightarrow 2c\text{-}YAl_2B_4O_{10.5} \quad (4)$$

$$3c\text{-}Al_4B_2O_9+4c\text{-}(Y,Er)BO_3+3a\text{-}B_2O_3\rightarrow 4c\text{-}(Y,Er)Al_3(BO_3)_4 \quad (5)$$

- 1050–1200°C

$$2a\text{-}AlBO_3+2c\text{-}YAl_2B_4O_{10.5}\rightarrow 2c\text{-}(Y,Er)Al_3(BO_3)_4+s\text{-}B_2O_3 \quad (6)$$

The small letter a indicates the 'amorphous phase', c indicates the 'crystalline phase' and s indicates the 'sublimation' of the boron oxide. On the basis of the initial stoichiometry, we could expect a B_2O_3 residual amorphous phase. But this residual B_2O_3 phase is lost through its partial sublimation. On the other hand, reactions (1) to (5) involve the presence of B_2O_3 in the amorphous remaining network. This further justify to initially involve a B_2O_3 excess to compensate its lost in temperature but also to favor the (1)–(5) reactions leading finally through reactions (5) and (6) to the pure Er:YAB synthesis.

The particle average size of the powder was estimated by TEM experiments. Figure 5 illustrates the images for amorphous powder heat treated at 400°C/24 h and 700°C/24 h (Fig. 5a) and crystalline powder heat treated at 400°C/24 h and 700°C/24 h and 1150°C/10 min (Fig. 5b). The amorphous powder presents average particle size lying between 50 and 100 nm while the crystalline powder exhibits parallelepiped form of around two and three hundreds of nanometers. In this case, it is possible to note some coalescence between the crystalline grains which indicates an initial sintering process.

Conclusions

A well-controlled complex synthesis and thermal treatments led to the formation of pure Er:YAB phase. Based on the thermal analyses and XRD results, several intermediate chemical reactions were specified. The Er:YAB crystalline phase was successfully obtained by addition of boron excess (boric acid precursor) in order to counter-balance the small boron loss observed during annealing between 800–1040°C. Nanometer-size powder presented some coalescence during heat treatment. Our results contribute to a better understanding of this complex system and open the route to obtain rare-earth doped YAB fine powders that is a crucial step for the preparation of ceramics and for the development of new phosphor compounds.

Acknowledgements

We gratefully acknowledge financial support from CAPES (No. 455/04/06), COFECUB, FAPESP and CNPq agencies.

References

1 N. Y. Leonyuk, E. V. Koporulina, S. N. Barilo, L. A. Kurnevich and G. L. Bychkov, J. Cryst. Growth, 191 (1998) 135.
2 N. I. Leonyuka, E. V. Koporulina, V. V. Maltsev, A. V. Mokhov and O. V. Pilipenko, J. Cryst. Growth, 281 (2005) 587.
3 E. Beregi, E. Hartmann, L. Malicsko and J. Madarász, Crys. Res. Technol., 34 (1999) 641.
4 E. V. Koporulina, N. I. Leonyuk, O. V. Pilipenko, A. V. Mokhov, G. Bocelli and L. Righi, Mater. Lett., 47 (2001) 145.
5 E. Beregi, A. Watterich, L. Kovács and J. Madarász, Vib. Spectrosc., 22 (2000) 169.
6 J. Madarász, E. Beregi, J. Sztatisz, I. Földvári and G. Pokol, J. Therm. Anal. Cal., 64 (2001) 1059.
7 S. T. Jung, J. T. Yoon and S. J. Chung, Mater. Res. Bull., 31 (1996) 1021.
8 L. J. Q. Maia, V. R. Mastelaro, S. Pairis, A. C. Hernandes and A. Ibanez, J. Solid State Chem., 180 (2007) 611.
9 L. J. Q. Maia, A. Ibanez, L. Ortega, V. R. Mastelaro and A. C. Hernandes, J. Nanopart. Res., 10 (2008) 1251.
10 M. L. Luetkens Jr. and B. L. C. Satek, US Patent no 5,043,308 Crystalline RE Aluminum Borates, (1991).

Received: October 9, 2007
Accepted: October 3, 2008

DOI: 10.1007/s10973-007-8821-1